

# Turbulence in exciton–polariton condensates

Natalia G. Berloff

*Department of Applied Mathematics and Theoretical Physics,  
University of Cambridge, Cambridge, CB3 0WA*

(Dated: 22 October 2010)

Nonequilibrium condensate systems such as exciton-polariton condensates are capable of supporting a spontaneous vortex nucleation. The spatial inhomogeneity of pumping field or/and disordered potential creates velocity flow fields that may become unstable to vortex formation. This letter considers ways in which turbulent states of interacting vortices can be created. It is shown that by combining just two pumping intensities it is possible to create a superfluid turbulence state of well-separated vortices, a strong turbulence state of de-structured vortices, or a weak turbulence state in which all coherence of the field is lost and motion is driven by weakly interacting dispersive waves. The decay of turbulence can be obtained by replacing an inhomogeneous pumping by a uniform one. We show that both in quasi-equilibrium and during the turbulence decay there exists an inertial range dominated by four-wave interactions of acoustic waves.

PACS numbers: 03.75.Lm, 71.36.+c, 03.75.Kk, 67.85.De, 05.45.-a

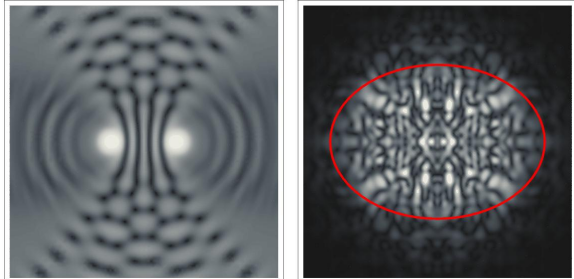
The phenomenon of turbulence – chaotic motion of vortices of many different length scales – is ubiquitous in nature, and quantitative understanding of it is a notoriously difficult problem of classical physics. Turbulence occurs in many usual fluid flows as well as in exotic systems such as plasmas and superfluids. Vorticity in superfluids is quantized in units of  $h/m$ , where  $m$  is the mass of the boson in contrast with continuously distributed vorticity of a classical Navier-Stokes fluid. In superfluid helium and weakly interacting Bose-Einstein condensates – superfluid systems in a thermodynamical equilibrium – quantized vorticity is considered to be an evidence for a macroscopically occupied quantum state that can be described by a classical complex-valued wave function  $\psi(\mathbf{x}, t)$ . On one hand, such quantization of velocity circulation in superfluids leads to significant differences between superfluid turbulence (ST) and classical turbulence. On the other hand, at large Reynolds numbers the motion of well-separated vortices in an incompressible classical flow may have similar features to ST. In this case the vortex dynamics in superfluids is almost classical in accordance with the Biot-Savart law, so that each vortex moves as a material line (a point in 2D) with the ambient flow and flow generated by other vortices. The decay of the turbulence (loss of the vortex line density) occurs due to dissipative effects induced by interactions with a normal fluid component (with a thermal cloud).

ST can be created in a number of ways (for review see e.g. [1]): in the counterflow of normal and superfluid components [2]; by injecting electron bubbles [3]; in the process of strongly non-equilibrium Bose-Einstein condensation (Kibble-Zurek effect) [4, 5]; by an external perturbation of the trap in atomic Bose-Einstein condensates [6]. In the latter by introducing an external oscillatory perturbation in the trap it became possible to obtain a disordered system of many topological defects. The dy-

namics of this matter field differs from both dynamics of vortices in classical turbulence and in superfluid helium turbulence. Firstly, the characteristic distance between vortices is comparable to their core sizes, so the chaotic behavior is seen on the level of a single vortex, secondly, these vortices are not structured, so they do not obey Biot-Savart Law, finally, the system is in a strongly non-equilibrium state. These create a novel nontrivial regime of a classical complex matter field — “strong turbulence” state – whose evolution is quite different from that of ordered condensate. In analogy with other nonlinear systems such as plasmas, fluids and nonlinear optics, apart from the regime of strong turbulence there should exist the regime of weak turbulence where all phases of the complex amplitudes of the matter field are random. This state has not been previously observed in cold atomic systems, but it plays crucial role in kinetics of Bose-Einstein condensation [4]. It has been suggested [7] that if even stronger external perturbation is applied to the trap, it is in principle possible to obtain a weak turbulence state where all phases of the complex amplitudes of the matter field are random. When this is done it will lead to a discovery of nontrivial regimes of classical matter fields in atomic systems.

In the last few years the Bose-Einstein condensation has been achieved in solid state systems [8], such as microcavities, ferromagnetic insulators and within superfluid phases of  $^3\text{He}$ . Microcavity exciton-polaritons are quasi-particles that consist of superpositions of photons in semiconductor microcavities and excitons in quantum wells. The Bragg reflectors confining photon component are imperfect, so exciton-polaritons have finite life time and have to be continuously re-populated. Such combination of pumping and decay leads to quasi-particle flow even at steady states of the system. At sufficiently low densities these quasi-particles can form a Bose-Einstein condensate, so the many particles quan-

FIG. 1: (color online) The time snapshots of the density  $|\psi|^2$  of the fields  $\psi$  obtained by numerical integration of Eq. (1) for  $\eta = 0, \sigma = 0.3$  and (i)  $\alpha(\mathbf{x}) = 2$  for  $|\mathbf{x} - (\pm 5, 0)| < 2$  and  $1/2$  otherwise,  $t=100$  (left panel) and (ii)  $V_{\text{ext}} = x^2 + y^2$  and  $\alpha(\mathbf{x}) = 5$  for  $x^2 + 2y^2 < 64$  and  $\alpha = -0.5$  otherwise (right panel). Red ellipse indicates the pumping spot. Luminosity of the density plots is proportional to density. Vortices are seen as black dots.



tum system can be represented by a classical complex-valued field  $\psi$  and so be described by a classical equation in a form of the complex Ginzburg-Landau equation (cGLE) [10, 11]:

$$2i\partial_t\psi = [-\nabla^2 + |\psi|^2 + i(\alpha - i\eta\partial_t\psi - \sigma|\psi|^2)]\psi, \quad (1)$$

where  $\alpha$  is an effective gain that represents intensity of the pumping field,  $\sigma$  represents nonlinear losses. The unit of length is a healing length  $\xi = \hbar/\sqrt{2mU\rho_\infty}$  that defines the size of the vortex core and the unit of time is  $\hbar/2U\rho_\infty$ , where  $U$  is the strength of a  $\delta$ -function interaction potential. We shall assume that  $\alpha = \alpha_0$  is constant away from some localised nonuniformities and so the number density there is  $\rho_\infty$ . It is possible to include a disorder potential of the microcavity by adding  $V_{\text{ext}}(\mathbf{x})\psi$  to the right-hand side of Eq. (1).

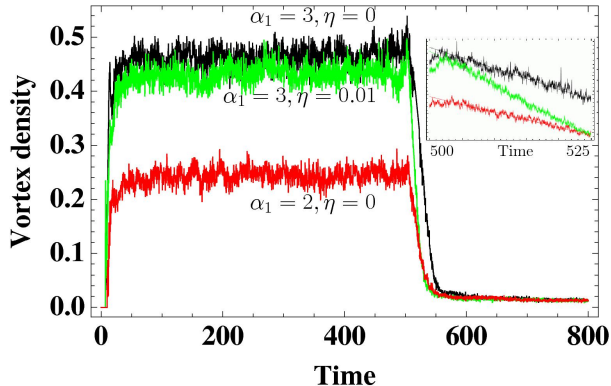
This equation is a mean-field description of the condensate; it can also be derived from the saddle point in a path integral formalism [12]. In the absence of pumping and dissipation Eq.(1) reduces to the Gross-Pitaevskii equation describing an equilibrium Bose-Einstein condensate. The energy relaxation has been noted to be of importance in experiments on extended 1D waveguides [13, 14]. These effects can be included in the cGLE by means on a parameter  $\eta$  [15]. This is the same term that has been incorporated into the Gross-Pitaevskii equation to represent a dissipation of the condensate component due to interactions with a thermal cloud [16]. The turbulence and mechanisms of the vortex generation in equilibrium condensates are well known. These include (i) interactions of finite amplitude sound waves (e.g. energy exchange between rarefaction pulses may lead to vortex formation) [17]; (ii) existence of critical velocities of the flow (e.g. moving objects generate vortices if the Landau critical velocity is reached on their surfaces [18]); (iii) modulational instabilities of density variations (e.g.

transverse instability of a dark soliton in 2D generates vortices) [19]. Some of these mechanism may produce vortices in the cGLE as well. For instance, the flow of exciton-polaritons about a spatially extended defect may produce vortex pairs of opposite circulation depending on the flow velocity [20]. In addition, Eq. (1) with gain and dissipation can form vortices by other physical mechanisms. For instance, an inhomogeneity of the pumping or/and disorder potentials form steady currents which may produce vortices through pattern forming symmetry breaking mechanism [10].

Although the formation of vortices has been observed in experiments [9] they seem to appear due to the intrinsic disorder potential in CdTe. The vortices become pinned at the local minimum of such potential and remain stationary. So the conditions in which a turbulent state of matter can be obtained in exciton-polariton condensates remained unclear. The purpose of this letter is to suggest how the turbulent state can be created in such a system and to study the properties and structure of the turbulence. It will be shown that turbulence can be created by deliberately designed pumping fields, and depending on characteristics of such fields the system can reach various regimes of turbulence from superfluid turbulence to strong and finally weak-turbulent state.

To illustrate the basic mechanism that drives the formation of vortices we first consider a pumping field in a form of a step function in 1D, so that  $\alpha = \alpha_1 + \alpha_0, \sigma = \sigma_1, \eta = \eta_1$  for  $x < 0$  and  $\alpha = \alpha_0, \sigma = \sigma_0, \eta = \eta_0$  for  $x > 0$ . The steady state mass continuity and Bernoulli equations resulting from the Madelung transformation  $\psi = \sqrt{\rho}\exp iS$  applied to Eq. (1) are  $\mu = u^2 + \rho - d^2\sqrt{\rho}/2\sqrt{\rho}dx^2$  and  $d(\rho u)/dx = (\alpha - \eta\mu - \sigma\rho)\rho$  where  $\rho$  is the number density,  $u = S'(x)$  is the velocity and the chemical potential  $\mu$  is introduced by  $2i\partial_t\psi = \mu\psi$ . Away from large density fluctuations we can drop the quantum pressure term  $d^2\sqrt{\rho}/2\sqrt{\rho}dx^2$ . We expect that  $u \rightarrow 0$  as  $x \rightarrow -\infty$ , so  $\mu \rightarrow (\alpha_1 + \alpha_0)/(\sigma_1 + \eta_1)$ . As  $x \rightarrow \infty$ , therefore, there will be a steady current  $u = [\alpha_1(\eta_0 + \sigma_0) + \alpha_0(\eta_0 - \eta_1 + \sigma_0 - \sigma_1)/\sigma_0(\eta_1 + \sigma_1)]^{-1/2}$  generated by the step. The presence of boundaries or other sources of outflow generate interference fringes seen, for instance, in recent experiments in 1D [13]. In 2D the fringes that meet at nonzero angles evolve into a pair of vortices of opposite circulation as seen on the left panel of Fig. (1). The mechanism leading to vortex formation in this case is analogous to the transverse instability of a density depletion in a conservative Gross-Pitaevskii equation [19]: the motion of grey solitons is inversely proportional to their depth, so modulation in the transverse direction forces different parts of the front to move with different velocities leading to vortex pair formation. This suggests that the several sources of such flows may continuously generate a large number of vortices leading to a turbulent flow. Another possibility to create a turbulent flow is related to the formation of vor-

FIG. 2: (color online) The evolution of the density of vortices as a function of time. For time  $t < 500$  the pumping is nonuniform as discussed in the text. At time  $t = 500$  the nonuniformity of the pumping field is removed and the vortex density decays linearly, as the inset shows.

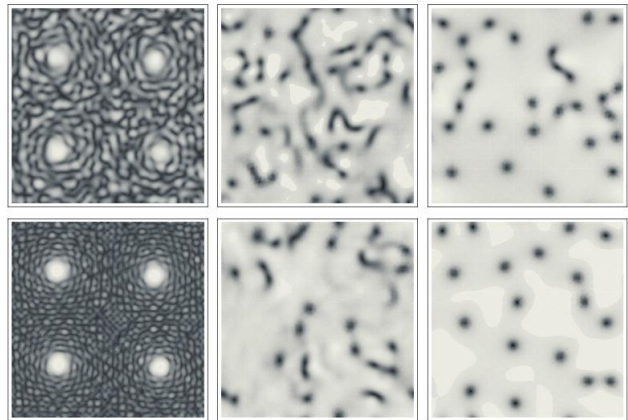


tex lattice in a harmonic trapping potential due to an instability of a non-rotating solution [10]. By removing the circular symmetry of either the trapping potential or pumping field it is possible to create a turbulent flow of vortices instead of a regular vortex lattice (see the right panel of Fig. 1).

In order to engineer a turbulent formation and interaction of vortices we shall consider an inhomogeneous pump  $\alpha(\mathbf{x})$  that can be obtained by passing the laser beam through a spatial phase modulator. This will be even further simplified by assuming that only two laser intensities are allowed: the background with a superimposed set of almost periodic spots of a higher intensity, so that  $\alpha(\mathbf{x}) = \alpha_0$  everywhere except for  $\mathbf{x}$  inside the circles  $|\mathbf{x} - \mathbf{a}_i|^2 < c_i$  where  $\alpha(\mathbf{x}) = \alpha_1 + \alpha_0$  and  $c_i = c + \chi_i$ ,  $\mathbf{a}_i = (a_1 \pm iT + \delta_i, a_2 \pm iT + \phi_i)$ ,  $T$  is the period of spots,  $c$  is the square of the spot radius,  $i = 0, 1, 2, \dots$  and  $\chi_i, \delta_i$  and  $\phi_i$  are random displacements of the order of the healing length. Both  $\eta$  and  $\sigma$  take different values for different pumping intensities. In practice, setting different values for these quantities does not change the qualitative behaviour of the system. In what follows both  $\eta$  and  $\sigma$  will be set to be constants across the fields. When we refer to a difference of pumping intensities as a parameter that defines different turbulent regimes, it should be understood that it is the difference between chemical potentials that the system is trying to establish in different regions that is driving the turbulence. For numerical simulations we used a fourth-order finite differences in space and fourth-order Runge-Kutta integration in time. The number of grid points in physical space was set to  $512^2$  for the physical domain  $D = [-20, 20]^2$  with doubly periodic boundaries. The initial state is always taken to be constant  $\psi = \alpha_0/(\sigma + \eta)$ ,  $c = 4$ ,  $a_i = 10$ ,  $T = 10$  [21].

Through the time evolution one can observe the formation of vortices until their number begins to fluctuate

FIG. 3: The time snapshots of the density  $|\psi|^2$  of the fields  $\psi$  at  $t = 450$  (left),  $t = 550$  (middle) and  $t = 650$  (right) for  $\alpha_1 = 2, \eta = 0$  (top row) and  $\alpha_1 = 4, \eta = 0.01$  (bottom row). The dimensions of the box shown are  $[-20, 20]^2$ . At time  $t = 500$  the pumping intensity was set to become uniform with  $\alpha_1 = 0$ . The top left panel represents the state of strong turbulence, the bottom left is in a weak turbulence state with  $g_2 \sim 2$ ; see the discussion in the main text. When the pumping field became uniform the turbulence in both cases decayed, with the number of vortices decaying faster for nonzero  $\eta$ .



about a constant value; see Fig. 2. The larger difference between the two pumping intensities,  $\alpha_1$ , leads to the faster outflows and a larger number of vortices generated. The relaxation has a negative effect on the number of vortices (compare the vortex densities for  $\alpha_1 = 3$  and  $\eta = 0$  or  $\eta = 0.01$  on Fig. 2). At time  $t = 500$  (well after the quasi-equilibrium is reached) we remove the nonuniformity of the pump by setting  $\alpha_1 = 0$ . After that the vortices start annihilating each other leading to the decay of the turbulence. This stage can be compared and contrasted with the wave turbulence of the Gross-Pitaevskii equation where the forcing and dissipation are at given momenta and so have a different physical meaning [22]. For instance the decay of the vortex density is linear (see the inset of Fig. 2) rather than logarithmic. A representative time evolution of the density fields is shown on Fig. 3.

In order to describe the turbulence in the Eq.(1) we shall assume that there exists an inertial range in the momentum space and that the role of pumping and dissipation is insignificant there. The evolution equation for the wave spectrum defined by  $\langle \psi_i \psi_j^* \rangle = n(\mathbf{k}_i) \delta(\mathbf{k}_i - \mathbf{k}_j)$ , where  $\mathbf{k}_i$  are discrete wave vectors, can be obtained by using a random phase approximation and expanding in small nonlinearity [23]. Two solutions of the evolution equation correspond to a thermodynamic equipartition of the total kinetic energy  $E = \int k^2 n_k d\mathbf{k}$ , so that  $n_k \sim k^{-2}$  and to an equipartition of the total number of particles  $N = \int n_k d\mathbf{k}$ , so that  $n_k \sim \text{const}$ . These correspond to the two limits of the Rayleigh-Jeans distribution

$T/(k^2 + \mu)$ , where  $T$  is the temperature.

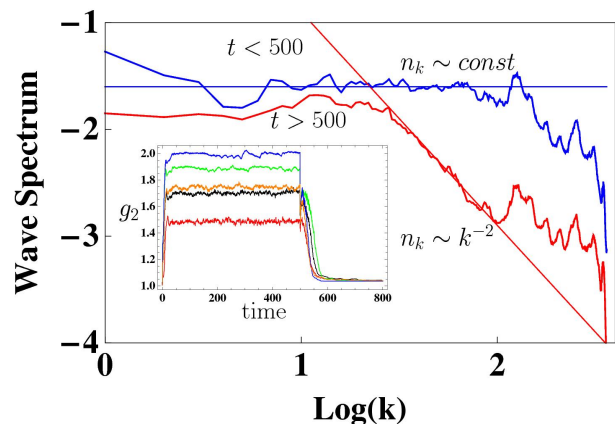
We verified the existence of the inertial range in our simulations. Although the system is in a quasi-equilibrium rather than in the true thermodynamical equilibrium we observed both spectra. For the nonuniform pumping the wave spectrum shows the particle equipartitions, during the turbulence decay stage the wave spectrum corresponds to energy equipartition (the Kolmogorov-Zakharov energy cascade  $n_k \sim k^{-2}$ ); see Fig. 4. This suggests that at these intermediate scales of the inertia range the turbulence is dominated by four-wave interactions and the wave field is weakly nonlinear and dominated by acoustic modes.

By tuning the nonuniformity of the pumping field it is possible to reach different turbulent regimes. If the difference between intensities,  $\alpha_1$ , is below a threshold or the distance between the spots of higher intensity is large, no vortices will be created. In a case of a moderate  $\alpha_1$  and only few spots a set of several well-formed well-separated vortex pairs is created and the system is in a superfluid turbulence state (see the left panel of Fig. 1). By increasing the difference between intensities  $\alpha_1$  it is possible to create the state of strong turbulence (where vortex cores start to overlap; see the top left panel of Fig. 3). It is, therefore, tempting to see if the system can be driven even further to enter the regime of weak turbulence in which all coherence is lost and all Fourier amplitudes have random phases. To verify this we calculated the second moment of the correlation function  $g_2 = D \int \rho^2 dx / (\int \rho dx)^2$ . By Wick's theorem the state of the weak turbulence corresponds to  $g_2 = 2$ . As shown on the inset to Fig. 4 by raising  $\alpha_1$  it is possible for the system to reach the weak turbulence state. Note that the relaxation  $\eta$  increases  $g_2$ . This occurs because the relaxation increases the rate at which vortex pairs annihilate by bringing the vortex cores closer to each other; this effect can be seen on Fig. 2 showing the number of vortices in quasi-equilibrium. The energy released from vortex annihilation becomes converted into acoustic energy therefore increasing  $g_2$ .

In summary, we proposed a way to generate various regimes of turbulence in nonequilibrium condensates, such as exciton-polariton condensates. By designing a nonuniform pumping field that leads to sufficiently strong interacting fluxes it is possible to create the superfluid turbulence with well separated quantised vortices, the strong turbulence with overlapping and de-structured vortices or the weak turbulence state with a complete loss of coherence. The nonequilibrium condensates, therefore, are new and exciting systems with a nontrivial evolution of complex matter field with turbulence that may span regimes fundamentally different from the classical fluid turbulence.

The author acknowledges useful discussions with A. Amo, C. Ciuti, J. Keeling and B. Svistunov.

FIG. 4: (color online) The wave spectrum  $\log(n_k)$  vs  $\log(k)$  for the state of strong turbulence established for parameters  $\eta = 0, \sigma = 0.3$  at  $t = 450$  (nonuniform pumping field with  $\alpha_1 = 3, \alpha_0 = 1/2$ , top blue curve) and at  $t = 650$  (uniform pumping field  $\alpha_1 = 0, \alpha_0 = 1/2$ , bottom red curve). Lines corresponding to  $n_k \sim \text{const}$  and  $n_k \sim k^{-2}$  are included. Inset shows the evolution of  $g_2$  in time for various  $\alpha_1$ . From bottom to top these graphs correspond to (i)  $\eta = 0, \alpha_1 = 2$ ; (ii)  $\eta = 0$  and  $\alpha_1 = 3$ ; (iii)  $\eta = 0.01, \alpha_1 = 3$ ; (iv)  $\eta = 0, \alpha_1 = 4$ ; (v)  $\eta = 0.01, \alpha_1 = 4$ . The top curve shows that the weak-turbulence state of turbulence is reached since  $g_2 \sim 2$ .



- [1] E. V. Kozik and B. V. Svistunov, *J. Low Temp. Phys.*, **156**, 215 (2009).
- [2] W. F. Vinen, *Proc. R. Soc. London, Ser. A* **240**, 114 (1957); *ibid.* **242**, 493 (1957); *ibid.* **243**, 400 (1957); K.W. Schwarz, *Phys. Rev. B* **31**, 5782 (1985); *ibid.* **38**, 2398 (1988); T.V. Chagovets, A.V. Gordeev, and L. Skrbek, *Phys. Rev. E* **76**, 027301 (2007).
- [3] P.M. Walmsley et al *Phys. Rev. Lett.* **99**, 265302 (2007).
- [4] N.G. Berloff and B.V. Svistunov, *Phys. Rev. A* **66**, 013603 (2002); and references therein.
- [5] C.N. Weiler et al *Nature* **455**, 948 (2008).
- [6] E. A. L. Henn, et al *Phys. Rev. Lett.* **103**, 045301 (2009)
- [7] N.G. Berloff and B.V. Svistunov *Physics* **2**, 61 (2009)
- [8] J.Kasprzak et al *Nature*, **443**, 409 (2006); R. Balili et al *Science*, **316**, 1007 (2007); A.Amo et al *Nature*, **457**, 291 (2009); S. Utsunomiya et al *Nature Phys.*, **4**, 700 (2008); A. Amo et al *Nature Phys.* (2009); S. O. Demokritov et al *Nature*, **443**, 430 (2006); V. E. Demidov et al *Phys. Rev. Lett.*, **100**, 047205 (2008); O. Dzyapko et al *Phys. Rev. B*, **80**, 060401(R) (2009); A.V.Chumak et al *Phys. Rev. Lett.*, **102**, 187205 (2009); Y. M. Bunkov and G. E. Volovik *Phys. Rev. Lett.* **98**, 265302 (2007); G. E. Volovik *J. Low Temp. Phys.*, **153**, 266 (2008).
- [9] K.G. Lagoudakis et al *nature Phys.*, **4**, 706 (2008).
- [10] J. Keeling and N. G. Berloff *Phys. Rev. Lett.*, **100**, 250401 (2008)
- [11] M. Wouters and I. Carusotto, *Phys. Rev. B*, **75**, 075332 (2007).
- [12] M. H. Szymańska et al *Phys. Rev. B*, **75**, 195331 (2007).
- [13] E. Wertz et al arXiv:1004.4084 (2010)
- [14] T. C. H. Liew et al arXiv:1008.5320 (2010).

- [15] M. Wouters and V. Savona, arXiv:1007.5431 (2010)
- [16] L.P.Pitaevskii *Sov. Phys. JETP*, **8**, 282 (1959).
- [17] N.G. Berloff, *J. Phys. A: Math. Gen.* **37**, 1617 (2004).
- [18] T. Frisch, Y. Pomeau, and S. Rica *Phys. Rev. Lett.* **69**, 1644 (1992); N.G. Berloff and P.H. Roberts *J. Phys. A: Math. Gen.*, **33**, 4025 (2000); T. Winiecki et al, *J. Phys. B: At. Mol. Opt. Phys.* **33**, 4069 (2000).
- [19] E. A. Kuznetsov and S. K. Turitsyn *Sov. Phys. JETP* **76**, 1583 (1988); E. A. Kuznetsov and J. J. Rasmussen *Phys. Rev. E* **51** 4479 (1995); N.S. Ginsberg, J. Brand, L.V. Hau, *Phys. Rev. Lett.* **94**, 040403 (2005); N.G. Berloff and C.F. Barenghi, *Phys. Rev. Letts.* **93** 090401(2004).
- [20] S. Pigeon et al, arXiv:1006.4755 (2010).
- [21] Numerically, the inhomogeneous pump consisting, for instance, of one spot will be represented by  $\alpha(\mathbf{x}) = \alpha_0 + \alpha_1(1 - \tanh(x^2 + y^2 - c))/2$ .
- [22] S. Nazarenko and M. Onorato *Physica D*, **219**, 1 (2006).
- [23] Z.E. Zakharov et al “*Kolmogorov Spectra of Turbulence*”, Springer-Verlag (1992).